Electronic Supplementary Information

Seven membered chelate Pt(II) complexes with 2,3-di(2-pyridyl)quinoxaline ligands: Studies of substitution kinetics by sulfur donor nucleophiles, interactions with CT-DNA, BSA and *in vitro* cytotoxicity activities

Rajesh Bellam,*[a] Deogratius Jaganyi,*[b,c] Allen Mambanda[a], Ross Robinson[a] and Manickam Dakshinamoorthi BalaKumaran[d]

[a]School of Chemistry and Physics, University of KwaZulu-Natal, Private Bag X01, Scottsville, Pietermaritzburg 3209, South Africa.
[b]School of Science, College of Science and Technology, University of Rwanda, P.O. Box 4285, Kigali, Rwanda.
[c]Department of Chemistry, Durban University of Technology, P.O. Box 1334, Durban 4000, South Africa.
[d]Department of Biotechnology, Dwaraka Doss Goverdhan Doss Vaishnav College, Arumbakkam, Chennai-600106, Tamil Nadu, India.

*Rajesh Bellam: rajeshchowdarybellam@gmail.com
*Deogratius Jaganyi: deojaganyi@gmail.com

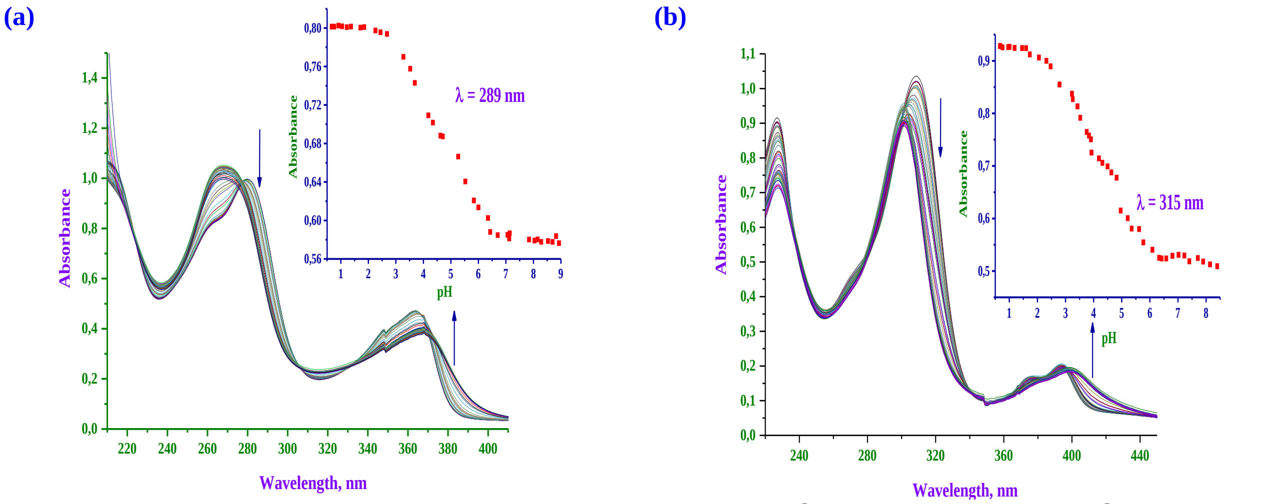

Fig. S1: UV-Vis. spectral changes of 50 μM **dmbpqPt(OH$_2$)$_2^{2+}$** (a) and **bbqPt(OH$_2$)$_2^{2+}$** (b) with pH range of 1-11; arrow indicates the change in the absorbance on the addition of TU. Inset: plot of absorbance *versus* pH at the specified wavelength (289 and 315 nm for **dmbpqPt(OH$_2$)$_2^{2+}$** and **dmbpqPt(OH$_2$)$_2^{2+}$**, respectively); I = 0.1 M (HClO$_4$) and T = 25 °C.

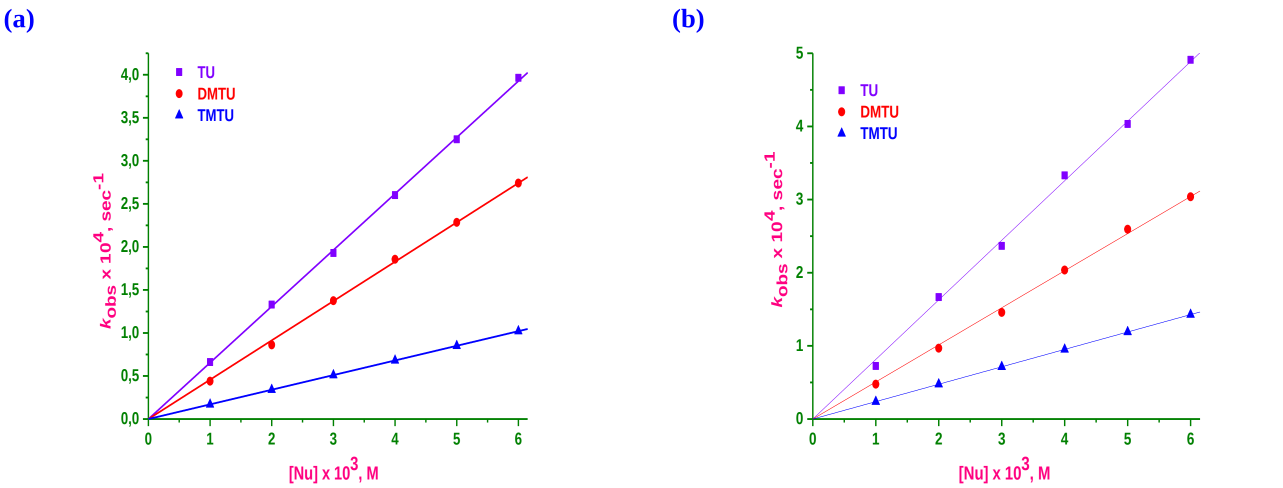

Fig. S2: Dependence plots of k_{obs} on [Nu] for the **dmbpqPt(OH$_2$)$_2^{2+}$** (a) and **bbqPt(OH$_2$)$_2^{2+}$** (b) with thiourea nucleophiles: [**dmbpqPt(OH$_2$)$_2^{2+}$ / bbqPt(OH$_2$)$_2^{2+}$**] = 50 μM, pH = 2.0, T = 35 °C and I = 0.1 M (NaClO$_4$).

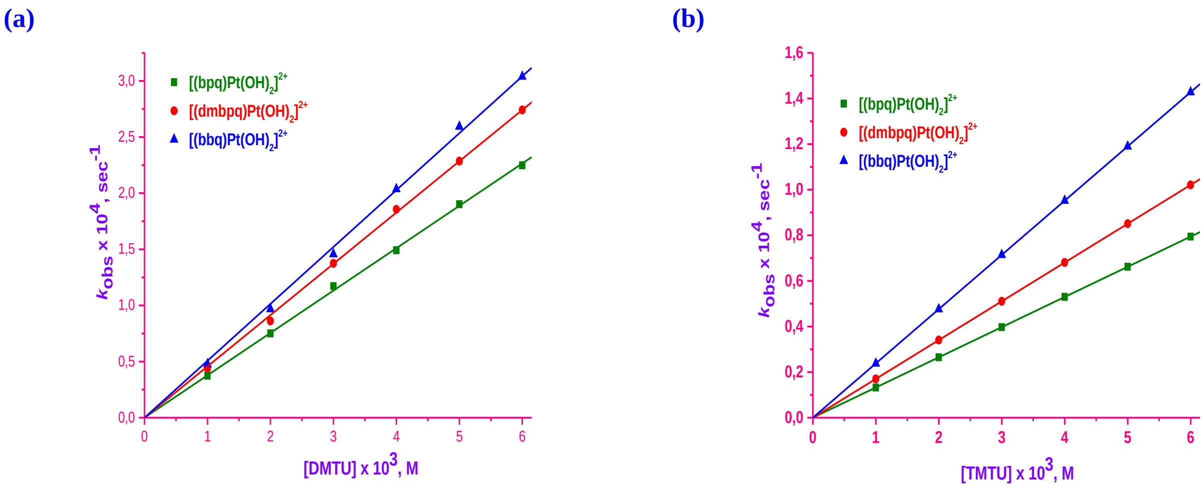

Fig. S3: Plots of k_{obs} on [DMTU] (a) and [TMTU] (b) for the three platinum complexes: [**dmbpqPt(OH$_2$)$_2^{2+}$ / bbqPt(OH$_2$)$_2^{2+}$**] = 50 µM, pH = 2.0, T = 35 °C and I = 0.1 M (NaClO$_4$).

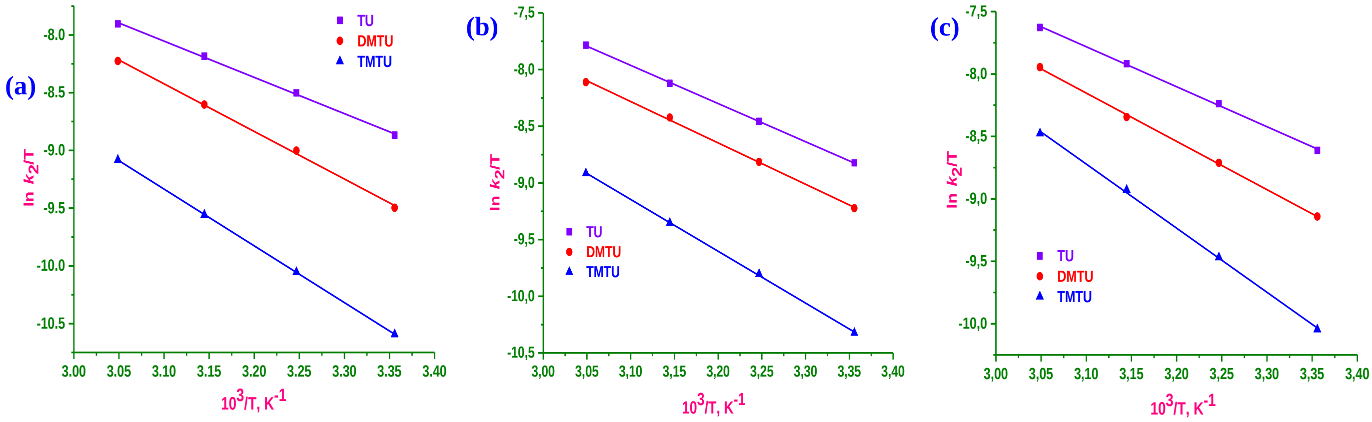

Fig. S4: Eyring plots for the substitution of aqua ligands of **bpqPt(OH$_2$)$_2^{2+}$** (a), **dmbpqPt(OH$_2$)$_2^{2+}$** (b) and **bbqPt(OH$_2$)$_2^{2+}$** (c) by S-donor nucleophiles.

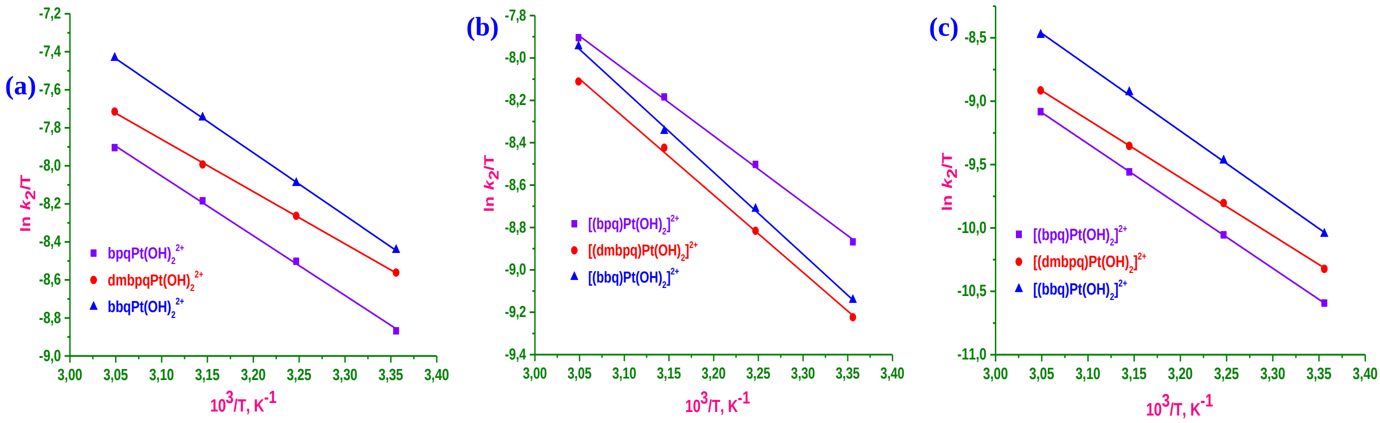

Fig. S5: Eyring plots for the substitution of aqua ligands of all the three Pt(II) complexes by TU (b), DMTU (b) and TMTU (c).

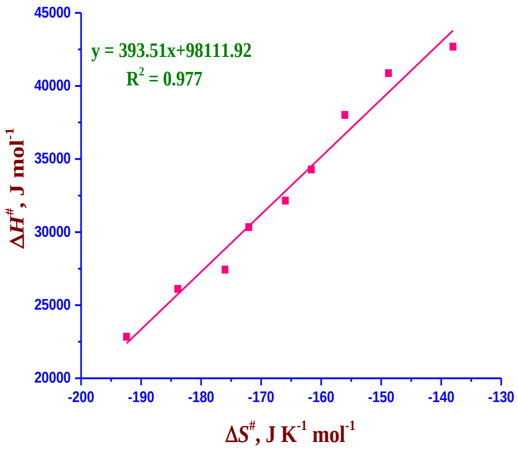

Fig. S6: *Iso*-kinetic plot for the aqua substitution reactions of Pt(II) complexes with S-donor nucleophiles.

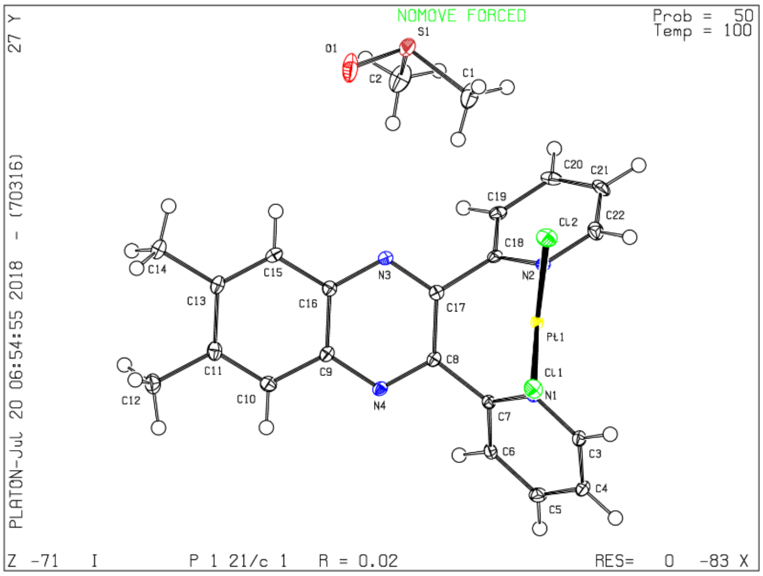

Fig. S7: ORTEP view and atom numbering scheme of the **dmbpqPtCl$_2$** complex with displacement ellipsoid at 50% probability.

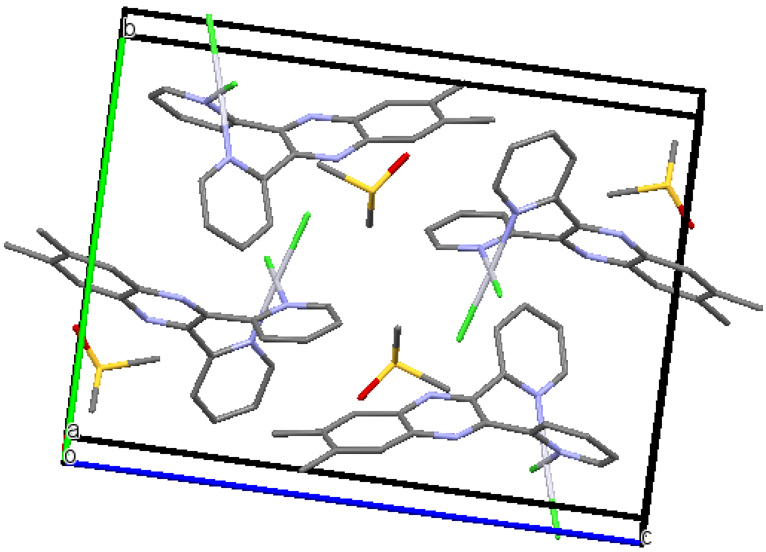

Fig. S8: Schematic packing diagram of the dmbpqPtCl$_2$ showing arrangement of the molecules of the complex, DMSO is also sketched. Hydrogen atoms are omitted for clear view.

Fig. S9: DFT-optimized structures, HOMO and LUMO maps for **bpq/dmbpq/bbqPt(OH)$_2^{2+}$** calculated by B3LYP/LANL2DZ method.

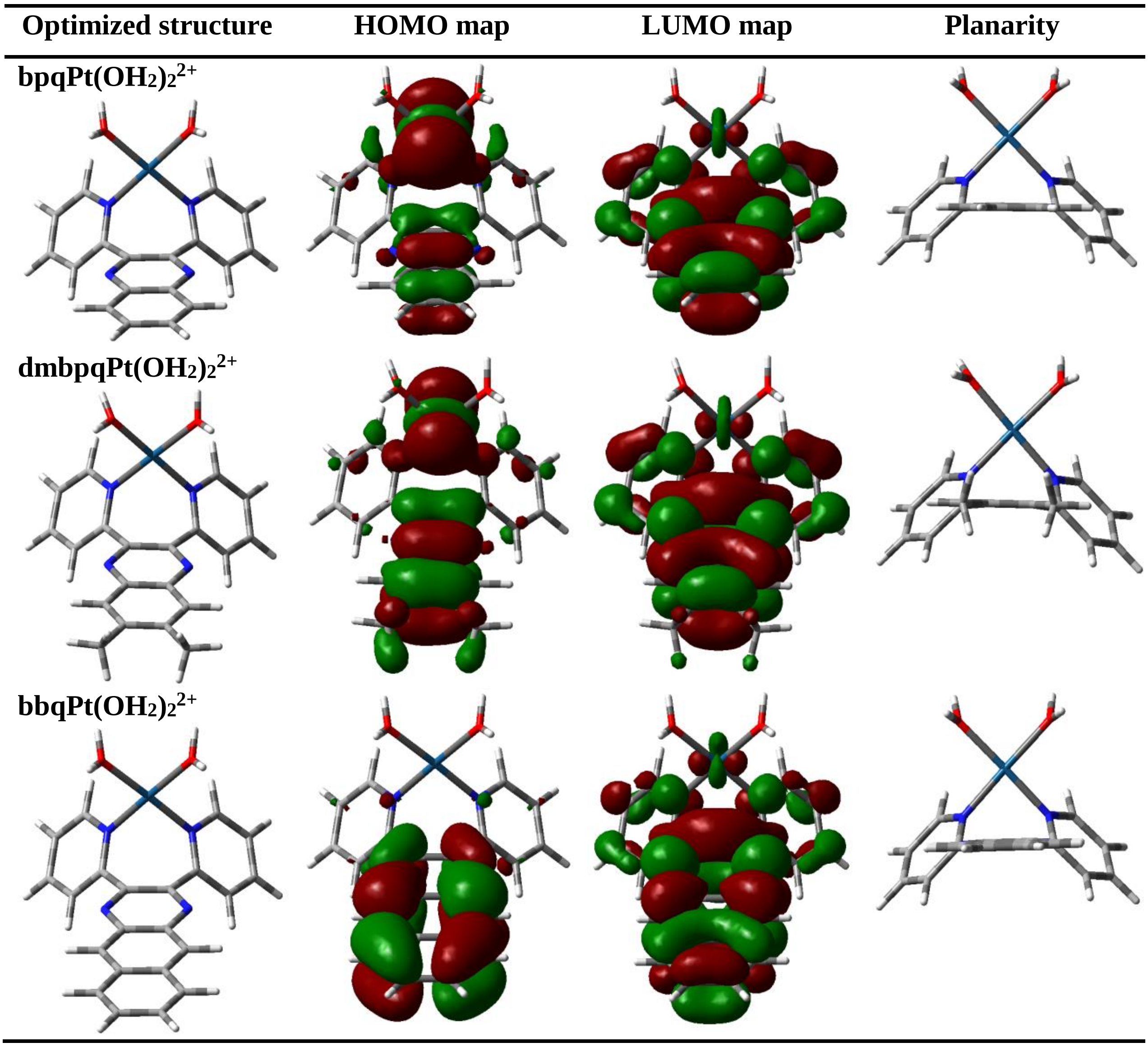

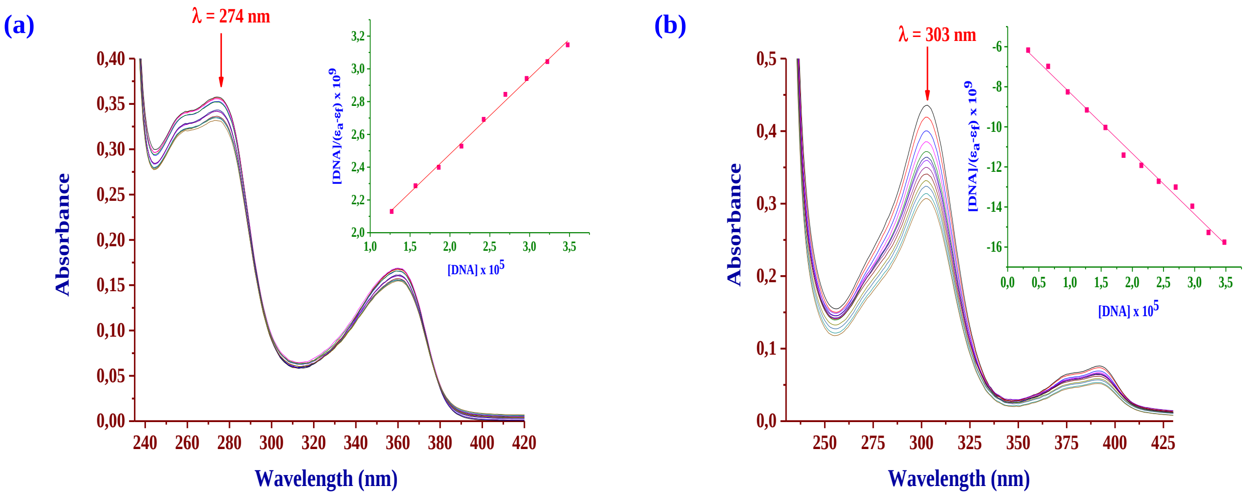

Fig. S10: Absorption spectra of 8 μM **bpqmePtCl$_2$** (a) and **bbqPtCl$_2$** (b) in Tris-HCl/50 mM NalCl buffer at pH 7.4) upon addition of CT-DNA (0-40 μM). The arrow shows the change in absorbance upon increasing the **CT-DNA** concentration. Inset: plot of [CT-DNA] versus [DNA]/(ε_a- ε_f).

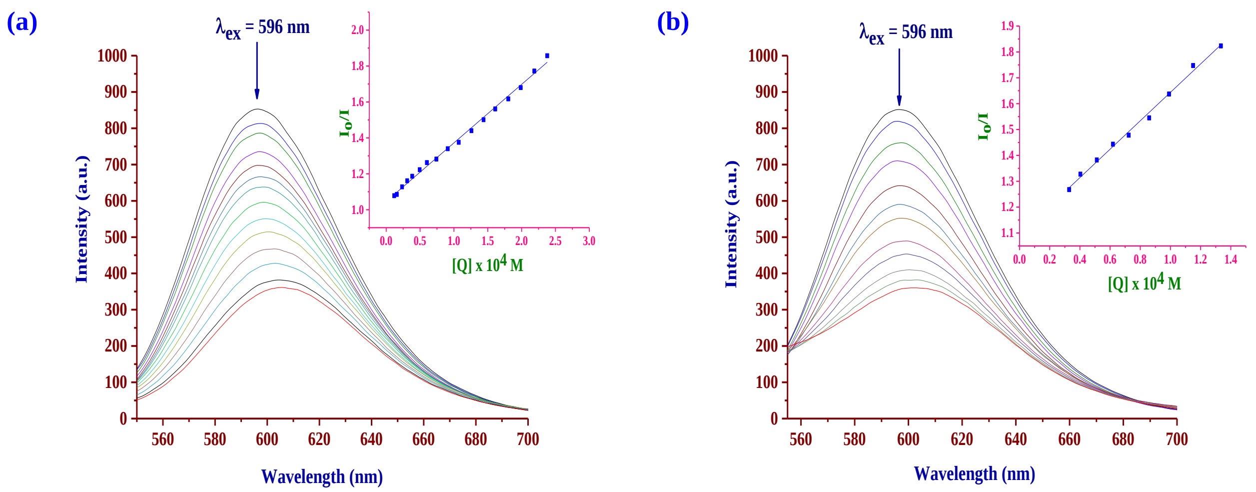

Fig. S11: Fluorescence emission spectra of EtBr bounded to CT-DNA in the presence **bpqmePtCl₂** (a) and of **bbqPtCl₂** (b): [EtBr] = 20 μM, [CTDNA] = 20 μM and [**bpqmePtCl₂/bbqPtCl₂**] = 0 - 300 μM. The arrow shows the intensity changes upon increasing the **bbqPtCl₂** complex concentration. Inset: Stern-Volmer plot of [Q] versus I_o/I.

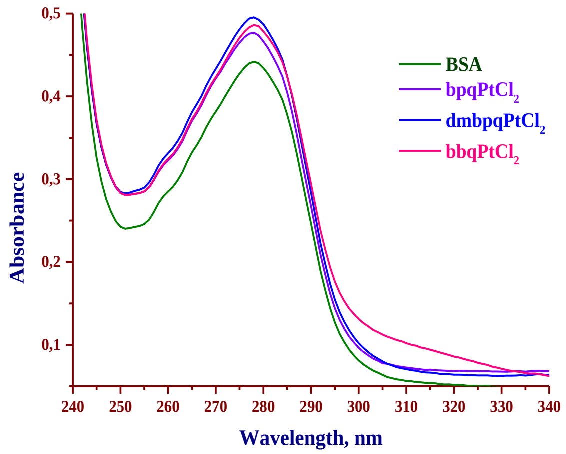

Fig. S12: Absorption spectra of 10 μM BSA with and without 5 μM of each Pt(II) complex.

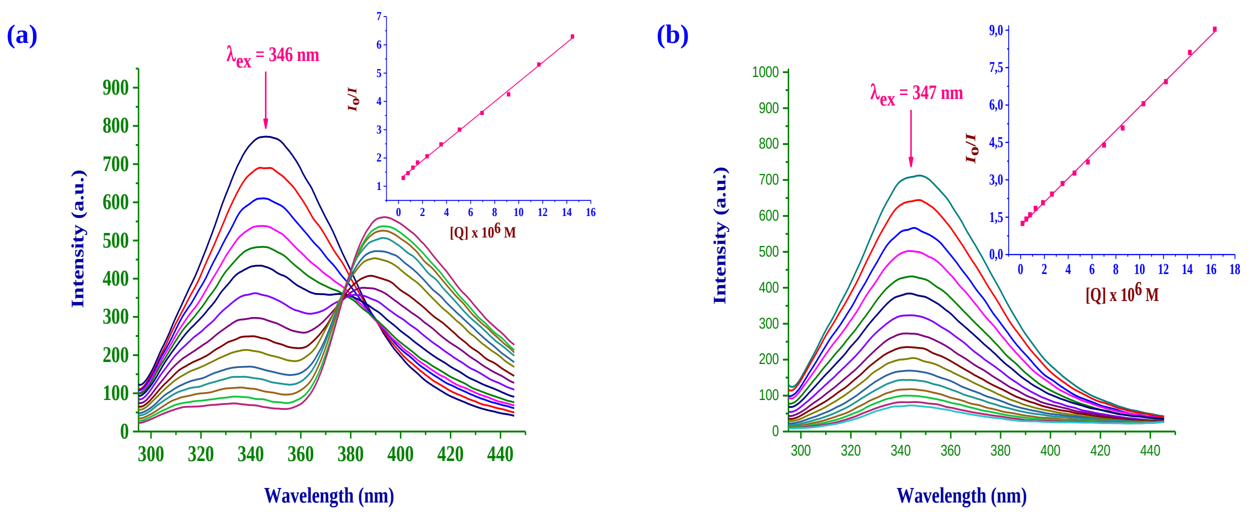

Fig. S13: Fluorescence emission spectra of BSA in the presence of **bpqmePtCl₂** (a) and of **bbqPtCl₂** (b): [BSA] = 1.2 μM and [**bpqmePtCl₂/bbqPtCl₂**] = 0 - 20 μM. The arrow shows the intensity changes upon increasing the complex concentration. Inset: Stern-Volmer plot of [Q] versus I_o/I.

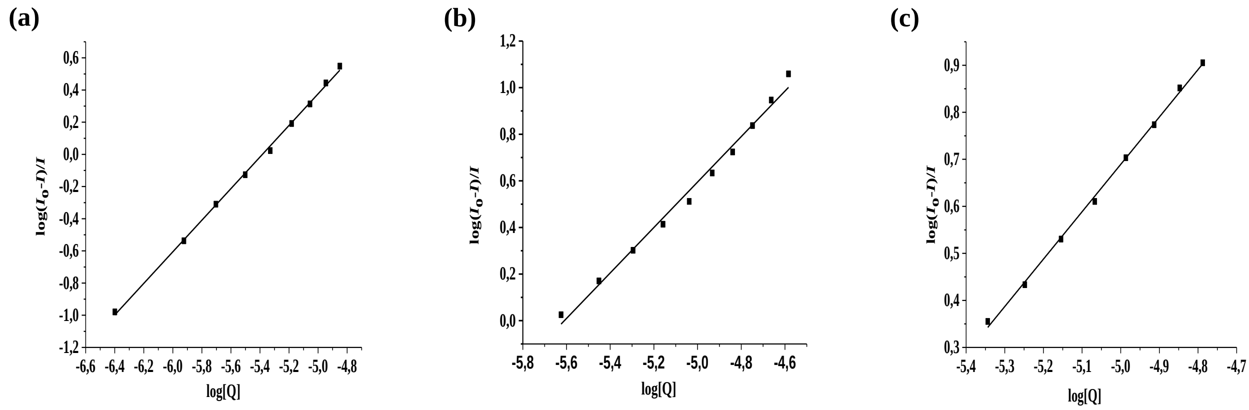

Fig. S14: Scatchard plots for the fluorescence quenching titration of BSA with increasing concentration of quencher; **bpqPtCl₂** (a), **bpqmePtCl₂** (b) and **bbqPtCl₂** (c).

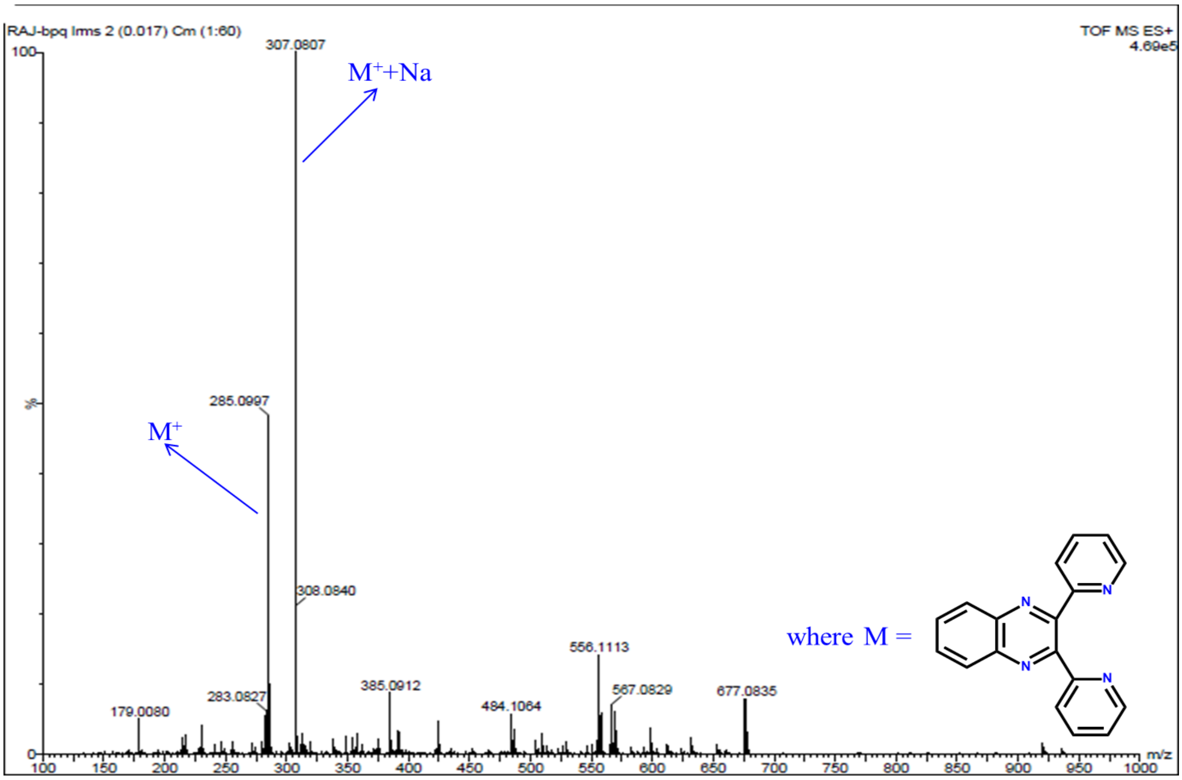

Fig. S15: TOF-MS spectra of 2,3-bis(2'pyriyl)-quinoxaline (bpq) ligand

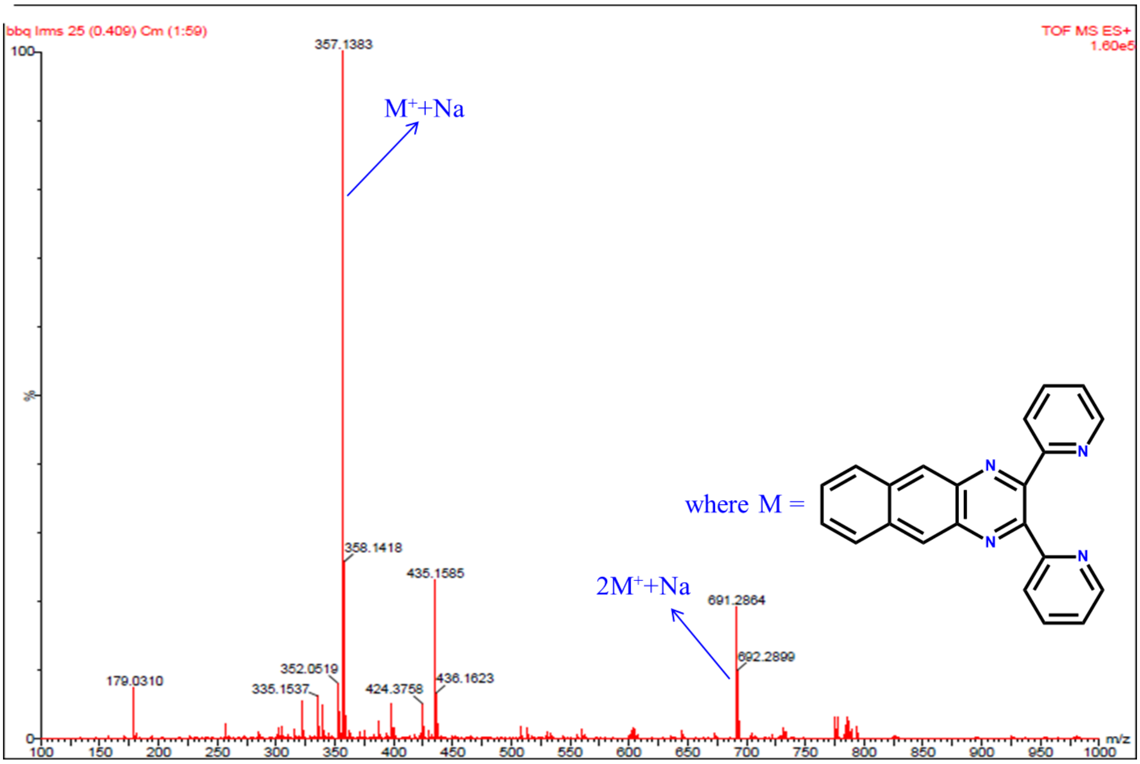

Fig. S16: TOF-MS spectra of 2,3-bis(2'pyriyl)benzo[g]quinoxaline (bbq) ligand

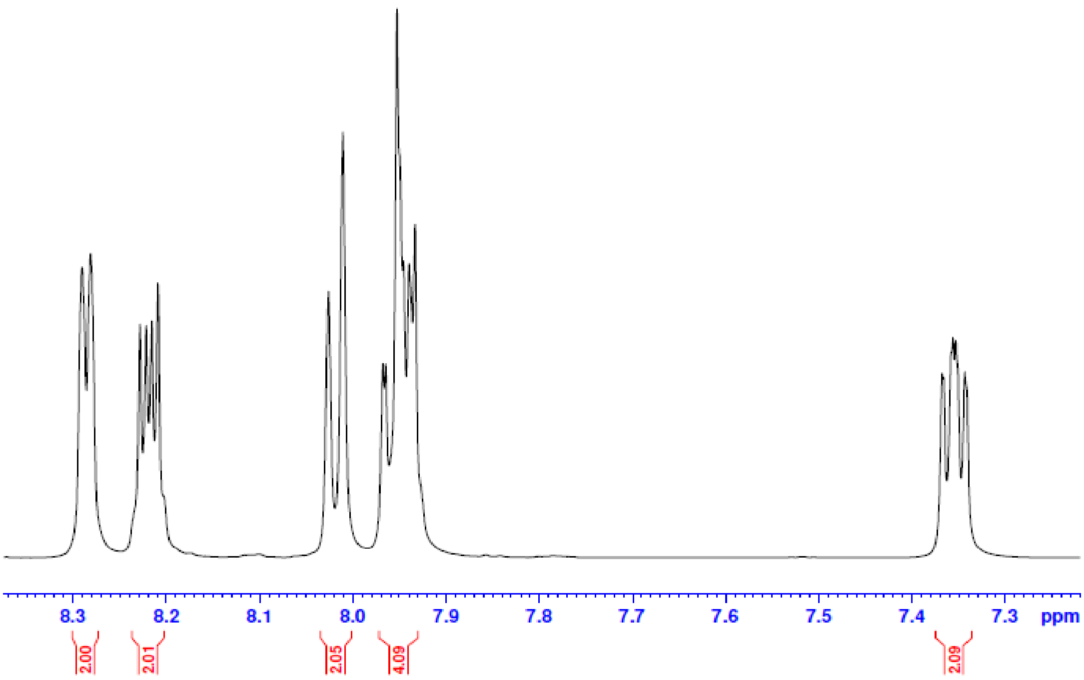

Fig. S17: ^{1}H NMR spectrum of 2,3-bis(2'pyriyl)-quinoxaline ligand (400 MHz, $(CD_3)_2SO$).

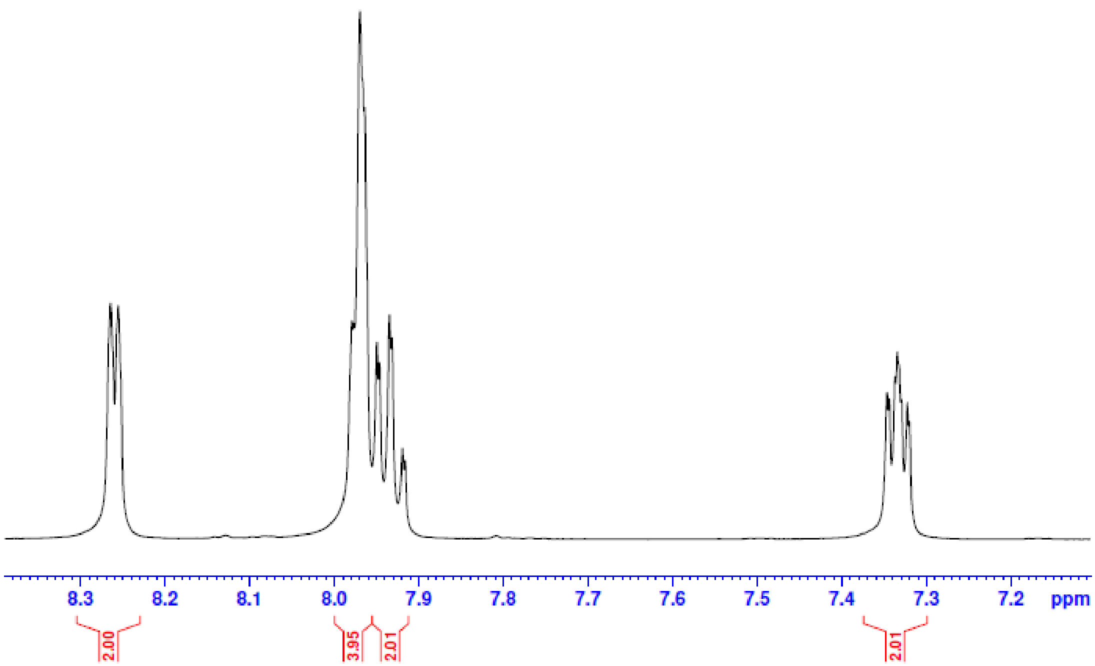

Fig. S18: ^{1}H NMR spectrum of 6,7-dimethyl-2,3-di(2-pyridyl)quinoxaline ligand (400 MHz, $(CD_3)_2SO$).

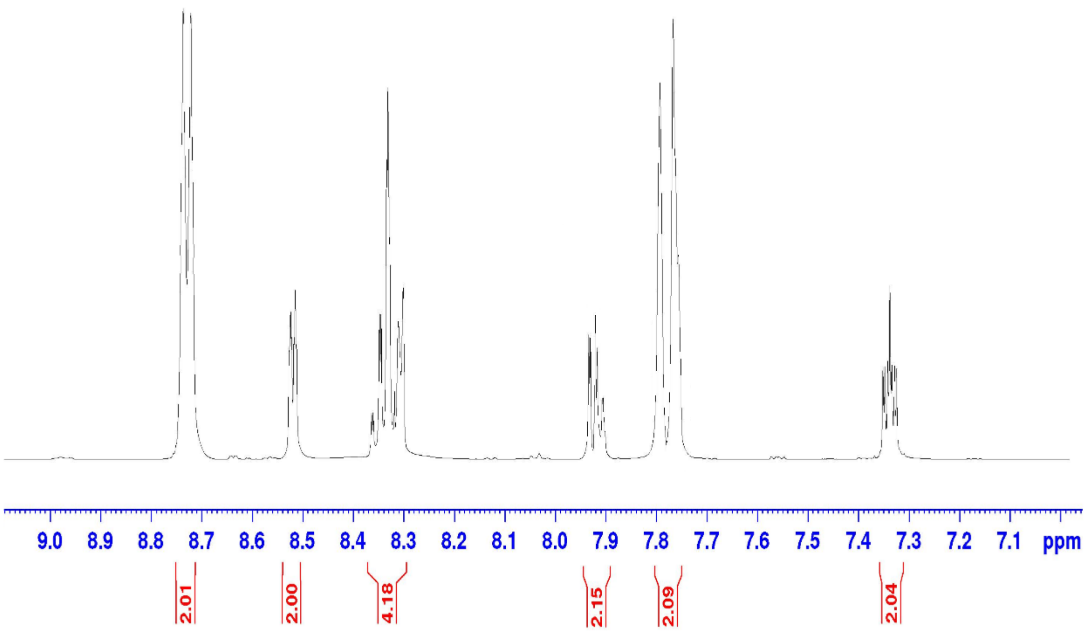

Fig. S19: ^{1}H NMR spectrum of 2,3-bis(2'pyriyl)benzo[g]quinoxaline ligand (400 MHz, $(CD_3)_2SO$).

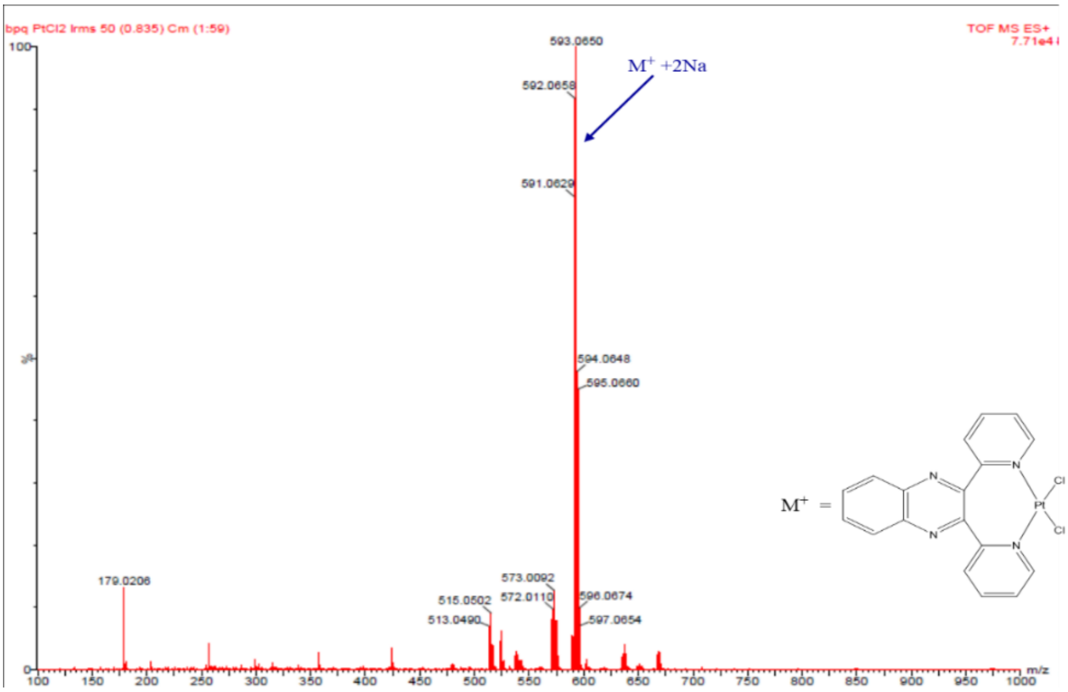

Fig. S19: TOF-MS spectra of 2,3-bis(2'pyriyl)-quinoxaline platinum (II) dichloride complex

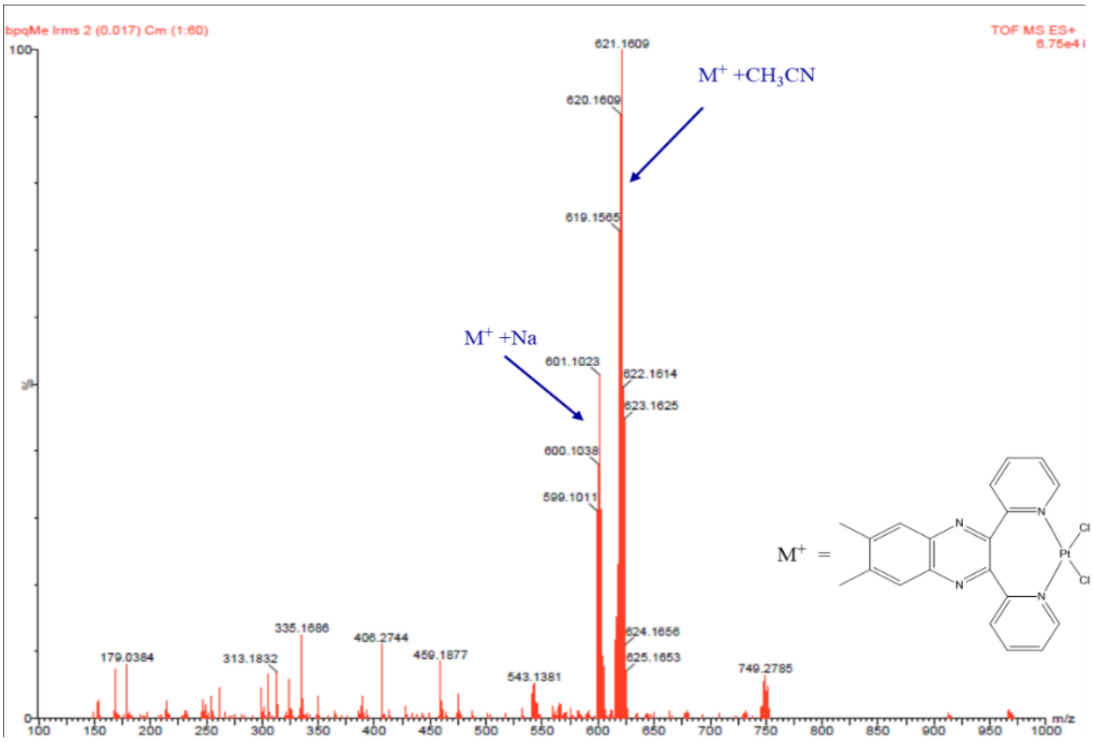

Fig. S20: TOF-MS spectra of 6,7-dimethyl-2,3-di(2-pyridyl)quinoxaline platinum (II) dichloride complex

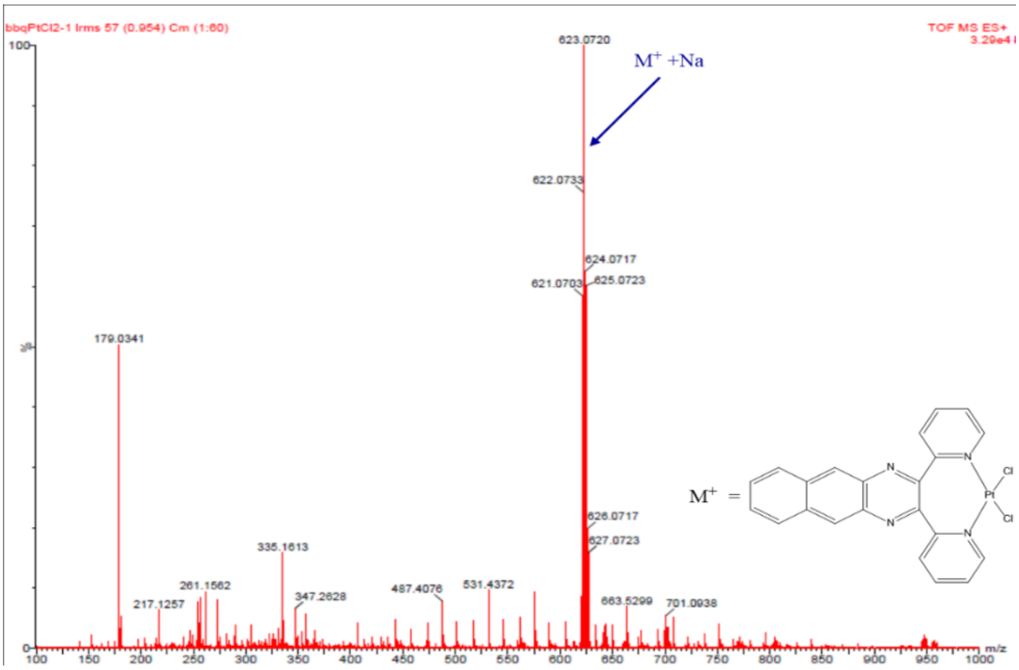

Fig. S21: TOF-MS spectra of 2,3-bis(2'pyriyl)benzo[g]quinoxaline platinum (II) dichloride complex

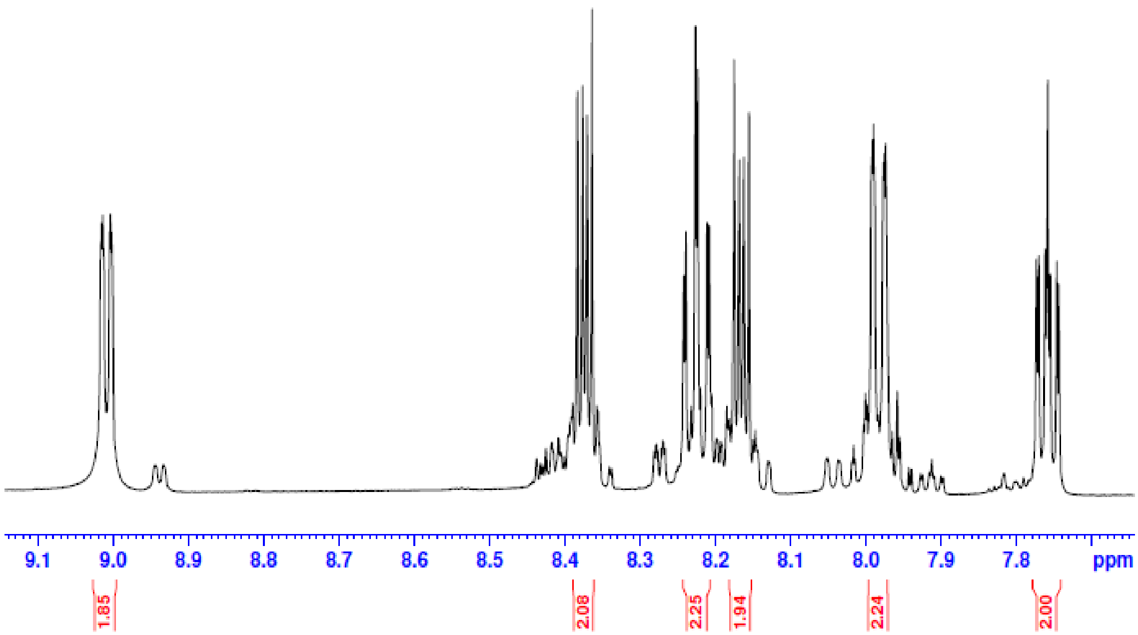

Fig. S22: ^{1}H NMR spectrum of 2,3-bis(2'pyriyl)-quinoxaline platinum (II) dichloride complex (400 MHz, $(CD_3)_2SO$).

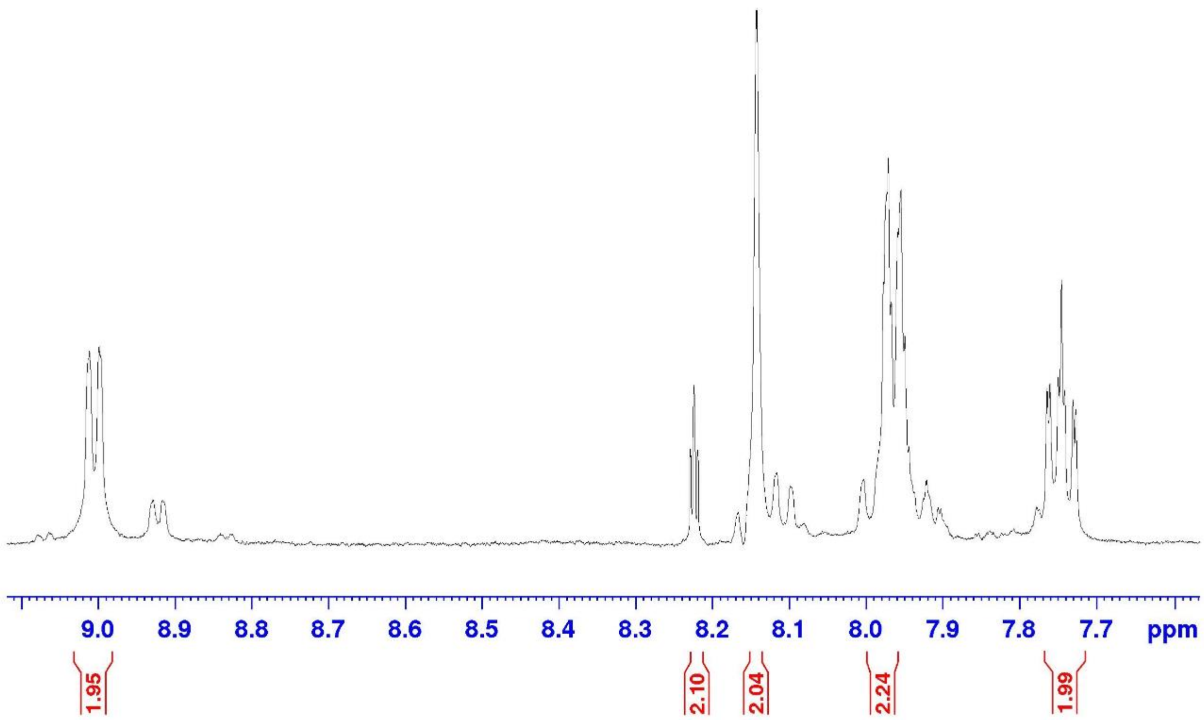

Fig. S23: ^{1}H NMR spectrum of 6,7-dimethyl-2,3-di(2-pyridyl)quinoxaline platinum (II) dichloride complex (400 MHz, $(CD_3)_2SO$).

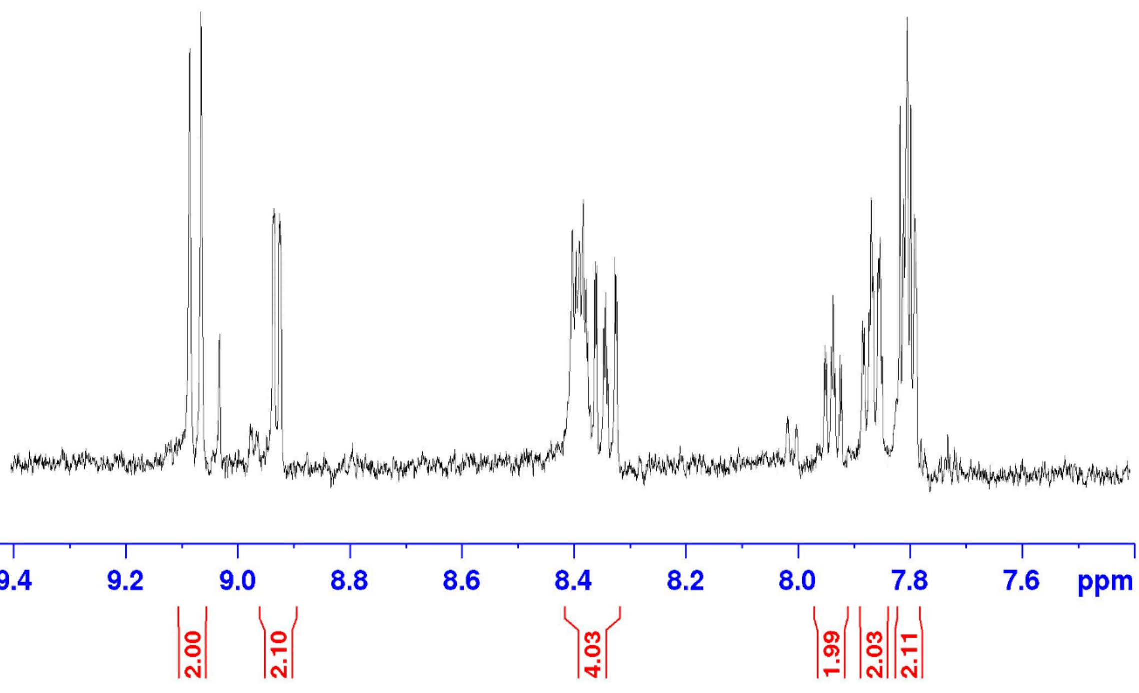

Fig. S24: ^{1}H NMR spectrum of 2,3-bis(2'pyriyl)benzo[g]quinoxaline platinum (II) dichloride complex (400 MHz, $(CD_3)_2SO$).

Table S1 λ_{max} in UV and Visible regions for both chloro and aquated Pt(II) complexes.

	Complex	λ_{max}	
		UV region	**Visible region**
Aqua	**$bpqPt(OH_2)_2^{2+}$**	274	343
	$dmbpqPt(OH_2)_2^{2+}$	278	363
	$bbqPt(OH_2)_2^{2+}$	303	393
Chloro	**$bpqPtCl_2$**	271	342
	$dmbpqPtCl_2$	274	360
	$bbqPtCl_2$	303	392

Table S2 Chosen wavelengths for kinetic traces to get k_{obs} values for the reactions of complexes with S-donor nucleophiles.

Complex	Nu	Wavelength, nm
$bpqPt(OH_2)_2^{2+}$	TU	292
	DMTU	292
	TMTU	292
$dmbpqPt(OH_2)_2^{2+}$	TU	300
	DMTU	300
	TMTU	313
$bbqPt(OH_2)_2^{2+}$	TU	304
	DMTU	304
	TMTU	406

Table S3 Summary of the second order rate constants, k_2 at 25, 45 and 55 °C for the substitution of aqua molecules by Nu.

Complex	Nu	k_2 x 10^2 / M^{-1} s^{-1}		
		25 °C	45 °C	55 °C
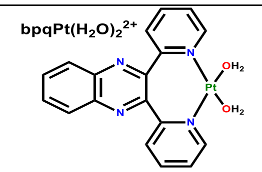	TU	4.20 ± 0.02	8.88 ± 0.09	12.11 ± 0.3
	DMTU	2.24 ± 0.02	5.84 ± 0.07	8.78 ± 0.1
	TMTU	0.75 ± 0.01	2.25 ± 0.05	3.73 ± 0.06
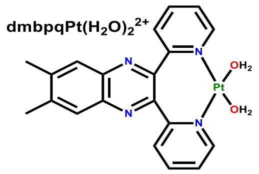	TU	5.70 ± 0.05	10.75 ± 0.2	14.64 ± 0.5
	DMTU	2.94 ± 0.03	6.99 ± 0.13	9.85 ± 0.3
	TMTU	0.98 ± 0.01	2.76 ± 0.07	4.41 ± 0.1
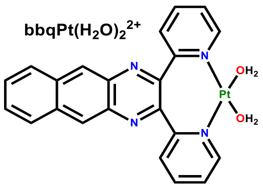	TU	6.42 ± 0.08	13.75 ± 0.5	19.41 ± 0.7
	DMTU	3.19 ± 0.06	7.56 ± 0.2	11.62 ± 0.5
	TMTU	1.29 ± 0.03	4.22 ± 0.1	6.83 ± 0.2

Table S4 Crystallographic data and structure refinement details for complex **dmbpqPtCl₂**

Parameter	**Values**
Empirical Formula	$C_{22}H_{22}Cl_2N_4OPtS$
Formula Wseven	656.48
Density ($D_{calc.}$), Volume (V)	1.943 g cm^{-3}, 2244.5(5) $Å^3$
Wavelength (λ), Absorption coefficient (μ)	0.71073 Å , 6.606 mm^{-1}
Shape, Colour	Block, Yellow
Temperature (*T*)	100(2) K
Z	4
Crystal Size	0.29×0.22×0.12 mm^3
Crystal System, Space Group	Monoclinic, $P2_1/c$
Unit Cell dimensions	a = 9.7436(13) Å α = 90°
	b = 13.0705(17) Å β = 93.454(4)°
	c = 17.656(2) Å γ = 90°
θ range for data collection	min. = 1.940° and max. = 27.499°
Transmissions (*T*)	min. = 0.589 and max. = 0.746
Reflections collected	26005
Independent Reflections	5153, [R_{int} = 0.0268]
Reflections with I > 2σ(I)	4832
Number of Parameters, Restrains	284, 0
Final *R* indices [I > 2σ(I)]	R_1 = 0.0154, wR_2 = 0.0337
Final *R* indices (all data)	R_1 = 0.0172, wR_2 = 0.0343
Goodness-of-fit on F^2	1.037
Largest Peak ($\rho_{max.}$), Deepest Hole ($\rho_{min.}$)	0.421, -0.339 e$Å^{-3}$

Table S5 DFT-calculated data for **bpq/dmbpq/bbqPt(OH$_2$)$_2^{2+}$** complexes

Complex		**bpqPt(OH$_2$)$_2^{2+}$**	**dmbpqPt(OH$_2$)$_2^{2+}$**	**bbqPt(OH$_2$)$_2^{2+}$**
MO energy (eV)				
I = -E_{HOMO}		7.204	7.088	6.372
A = -E_{LUMO}		2.803	2.954	3.298
$\Delta E_{LUMO-HOMO}$		4.401	4.134	3.074
NBO charge				
Pt^{2+}		0.839	0.840	0.844
Pyridyl N-atoms	N_1	-0.481	-0.483	-0.481
	N_4	-0.481	-0.484	-0.481
Quinoxaline N-atoms	N_2	-0.458	-0.463	-0.454
	N_3	-0.458	-0.462	-0.454
Bond lengths (Å)				
Pt-(OH$_2$)$_1$		2.0972	2.0982	2.0993
Pt-(OH$_2$)$_2$		2.0972	2.0984	2.1022
Pt-N_1		2.0092	2.0089	2.0085
Pt-N_4		2.0092	2.0087	2.0084
Chemical hardness (η)		2.201	2.067	1.537
Chemical softness (σ)		0.454	0.484	0.651
Electrophilicity index (ω)		5.652	6.099	7.605
Dipole moment (D)		12.54	13.80	17.18

Synthesis of ligands

2,3-bis(2'pyriyl)-quinoxaline, bpq

A solution of 2,2'-pyridil (1.06 g, 5 mmol) in ethanol was added to solution of *O*-phenylenediamine (0.54 g, 5.0 mmol) in ethanol and the mixture was refluxed for 1 h under constant stirring. Unreacted material was removed by filtration of the hot solution from which a light brown coloured product was separated on cooling. The product was collected by Millipore filtration and recrystallized from hot ethanol.

2,3-bis(2'pyriyl)benzo[g]quinoxaline, bbq

A mixture of ethanol solutions of 2,2'-pyridil (0.531 g, 2.5 mmol) and 2,3-Diaminonaphthalene (0.396 g, 2.5 mmol) were refluxed for 1 h under constant stirring. The volume was reduced to half by rotary evaporation and filtered. A crystalline product was formed on cooling the filtrate for 48 h. The product was filtered and recrystallized from hot ethanol.

Synthesis of dichloro platinum(II) complexes

A 20 mL stirring acetonitrile solution of $[Pt(DMSO)_2Cl_2]$ (211.13 mg, 0.5 mmol) and bpq (142.16 mg, 0.5 mmol) / dmbpq (156.19 mg, 0.5 mmol) / bbq (167.19 mg, 0.5 mmol) was heated in a light protected flask at about 70 ^{o}C for 2 h. Light yellow coloured precipitate which formed were filtered off, washed several times with small portions of acetonitrile and diethyl ether. The collected precipitates were dried under vacuum.

Preparation of diaqua platinum(II) complexes

An almost stoichiometric amount of $AgClO_4$ was added to the chloro complex, i.e., 1.98 to avoid Ag^+ encroachment in the aqua solutions. A suspension of **bpqPtCl₂** (82.55 mg, 0.15 mmol) / **dmbpqPtCl₂** (86.75 mg, 0.15 mmol) / **bbqPtCl₂** (90.05 mg, 0.15 mmol) and silver perchlorate (61.57 mg, 0.297 mmol) in 50 mL of 0.1 M perchloric acid ($HClO_4$) were heated for 24 h at 50 ^{o}C in dark. The AgCl precipitate which formed was removed by Millipore filtration system using 0.45 μm pore size nylon membrane.

pK_a determination of the aqua complexes

The aqua complexes were dissolved in a pH 1.0 solution of $HClO_4$ and the absorbance changes were monitored as the aqua complexes were titrated with NaOH. Incremental solid and solutions of NaOH were added to diaqua Pt(II) complex solution under vigorous stirring. To avoid dilution effects, crushed NaOH was used initially in the pH range of 1–2.5 after which dropwise addition of 0.5 M, 0.1 M and 0.05 M of NaOH solutions were made from a pipette dropper in order to get the pH change of less than 0.2 per each increment. After each addition of the base the complex solution, about 2 mL aliquots were taken in ampoules to measure pH. After determining the pH the samples in the ampoules were discarded to avoid possible chloride ion contamination from the pH electrode that was filled with saturated KCl solution.[1] For each increment in pH less than 3.0 mL of complex solution was placed in a cuvette for the record the absorption spectra. These solutions were retained titration vessel after recording. The plots of absorbance versus pH at a specific wavelength were fitted to double sigmoidal functions by the Boltzmann equation using the OriginPro 9.1® software.[2] The p*K*a values are calculated as an inflection point to filled data.

Preparation of complex and nucleophile solutions for kinetic analysis

Requisite volume of prepared diaqua Pt(II) complex was transferred into a volumetric flasks and filled-up to mark using 0.01 M $HClO_4$ (pH = 2.0) and $NaClO_4$ (0.1 M). A pH of 2 ensured that the complexes existed in the aqua form and $NaClO_4$ was used to maintain ionic strength. Requisite quantities of S-donor nucleophiles were also prepared in pH 2.0 (0.01 M $HClO_4$ and 0.1 M $NaClO_4$) solution. The nucleophile concentration was provided in at least 20-fold excess over that of the diaqua Pt(II) complex at 20; 40; 60; 80; 100 and 120 times higher concentrations to that of the aqua complexes. This afforded a ten-fold excess of the nucleophile concentration for each of the two coordinated leaving groups. This was to ensure that pseudo-first-order conditions were maintained at all times.

Kinetic procedure

All the kinetic runs were monitored using the scanning kinetics mode of the UV-Visible spectrophotometer, which records continuous spectral changes of the diaqua Pt(II) complexes after mixing with nucleophiles, over a period of time. Kinetics were performed at four different temperatures at 10 ^{o}C increment (25, 35, 45 and 55 ^{o}C) under pseudo-first-order conditions at a constant pH of 2.0 and ionic strength of 0.1 M. All the kinetic runs were performed in triplicate and the rate constants were reproducible within ± 3%. Suitable wavelengths for kinetic traces were chosen from reaction spectra and these are given in ESI table 3. The kinetic traces at selected wavelengths were fitted to a double exponential function of OriginPro 9.1® graphical analysis software[2] which gives p*seudo*-first-order rate constants, k_{obs}.

Molecular docking

The program uses Spherical Polar Fourier (SPF) correlations to accelerate the calculations. The coordinates of all Pt(II) complexes were optimized by the Gaussian 09 program and converted to PDB format using Mercury 3.3 software.[3] The crystal structure of the B–DNA dodecamer $d(CGCGAATTCGCG)_2$ (PDB ID: 1DNA) was retrieved from the protein data bank.[4] The docked pose of 1BNA and each complex were viewed using CHIMERA software.[5] The docking protocol was repeated three times and almost similar docking poses were viewed in each of the runs. The $E_{(lowest\ energy\ pose)}$ value of each dichloro Pt(II) complexes with DNA interactional poses were evaluated.

DNA binding studies

Absorption spectral studies

A fixed 20 μM concentration of each dichloroPt(II) complex (**bpqPtCl$_2$**, **dmbpqPtCl$_2$** and **bbqPtCl$_2$**) was titrated spectrophotometrically with increasing CT-DNA concentration (0 - 20 μM). The absorption spectra were obtained by adding the requisite amount of CT-DNA to both reference and sample solutions to eliminate the absorbance of CT-DNA. The Pt(II) complex-DNA solutions were allowed to incubate for 10 minutes in cuvette before the absorption spectra were recorded. The absorption changes were monitored at the MLCT bands of the complexes as a function of increasing concentration of CT-DNA. The binding affinities of the Pt(II) complexes were calculated using the Wolfe-Shimer equation (1).[6]

$$[DNA]/(\varepsilon_a - \varepsilon_f) = [DNA]/(\varepsilon_b - \varepsilon_f) + 1/(K_b(\varepsilon_b - \varepsilon_f)) \quad (1)$$

where [DNA] is the concentration of CT-DNA, ε_a, ε_f and ε_b are the molar absorptivities of the titrated mixture (A_{obs}/[complex]), unbound Pt(II) complex and the Pt(II)/CT-DNA complex, respectively. K_b is calculated from the ratio of the slope to intercept in the plot of $[DNA]/(\varepsilon_a - \varepsilon_f)$ versus [DNA].

Fluorescence spectral studies

Before recording the spectra, the solutions were thoroughly mixed and incubated for 10 minutes at room temperature. The quenching efficiency of the complexes was analysed using the Stern-Volmer equation (2).[7]

$$I_o/I = 1 + K_{sv}[Q] = 1 + k_q\tau_0 \quad (2)$$

where I_o and I are the emission intensities of CT-DNA+EtBr complex in the absence and each addition of complex, respectively and [Q] is the concentration of quencher (dichloro Pt(II) complex). The Stern-Volmer (quenching) constant, K_{sv} was determined from the slope of the linear plot of I_o/I versus [Q]. To have an insight on the kinetics of the competitive binding process, the bimolecular quenching rate constant, k_q values were also computed using the Stern-Volmer equation, where τ_0 is the average fluorescence lifetime of the CT-DNA+EtBr complex in the absence of the quencher and its value is 23 nanoseconds at room temperature.[8] The apparent binding constant, K_{app} was computed from the equation (3)

$$K_{EtBr}[EtBr] = K_{app}[Q] \quad (3)$$

where [Q] is the concentration of quencher causing 50 % reduction in fluorescence intensity of CT-DNA+EtBr complex, K_{EtBr} = 1.0 x 10^7 M^{-1} [9] and [EtBr] was taken as 320, 260 and 170 μM for **bpqPtCl₂**, **dmbpqPtCl₂** and **bbqPtCl₂**, respectively.

Bovine Serum Albumin (BSA) binding studies

Each spectrum was recorded after an incubation time of 10 minutes. The quenching efficiency of the Pt(II) complexes was calculated using the Stern-Volmer equation (2) as discussed above. The Stern-Volmer (quenching) constant, K_{sv} was determined from the slope of the linear plot of I_o/I versus [Q]. To have an insight on the kinetics of the competitive binding process, the bimolecular quenching rate constant, k_q values were also computed using the same Stern-Volmer equation (2), where τ_0 is the average fluorescence lifetime of the BSA alone is 6.13 nano seconds.[10] Scatchard plots also gave the binding constant K_F as determined from the fluorescence titration using Scatchard equation (4).

$$\log(I_o - I) / I = \log K_F + n \log[Q] \quad (4)$$

where n is representing the number of binding sites per nucleotide.

References:

1. D. Jaganyi, A. Hofmann and R. van Eldik, *Angew. Chem. Int. Ed.*, 2001, **40**, 1680-1683.
2. OriginPro 9.1. OriginLab Corporation, One Roundhouse Plaza, suite 303, Northampton, MA 01060, USA, 1800-969-7720.
3. C. F. Macrae, I. J. Bruno, J. A. Chisholm, P. R. Edgington, P. McCabe, E. Pidcock, L. Rodriguez-Monge, R. Taylor, J. v. d. Streek and P. A. Wood, *J. Appl. Crystallography*, 2008, **41**, 466-470.
4. H. R. Drew, R. M. Wing, T. Takano, C. Broka, S. Tanaka, K. Itakura and R. E. Dickerson, *Proc. Natl. Acad. Sci.*, 1981, **78**, 2179-2183.
5. E. F. Pettersen, T. D. Goddard, C. C. Huang, G. S. Couch, D. M. Greenblatt, E. C. Meng and T. E. Ferrin, *J. Comput. Chem*, 2004, **25**, 1605-1612.
6. A. Pyle, J. Rehmann, R. Meshoyrer, C. Kumar, N. Turro and J. K. Barton, *J. Am. Chem. Soc.*, 1989, **111**, 3051-3058.
7. O. Stern and M. Volmer, *Phys. Z*, 1919, **20**, 183-188.
8. D. P. Heller and C. L. Greenstock, *Biophys. Chem.*, 1994, **50**, 305-312.
9. M. Lee, A. L. Rhodes, M. D. Wyatt, S. Forrow and J. A. Hartley, *Biochem.*, 1993, **32**, 4237-4245.
10. E. Alarcon, A. Aspée, M. Gonzalez-Bejar, A. Edwards, E. Lissi and J. Scaiano, *Photochem. Photobiol. Sci.*, 2010, **9**, 861-869.
11. U. Anand, C. Jash and S. Mukherjee, *Phy. Chem. Chem. Phy.*, 2011, **13**, 20418-20426.